

Synthesis of uniform hollow silica spheres with ordered mesoporous shells in a CO₂ induced nanoemulsion

Yueju Zhao, Jianling Zhang, Wei Li, Chaoxing Zhang, Buxing Han*

Beijing National Laboratory for Molecular Sciences, Institute of Chemistry, Chinese Academy of Sciences, Beijing
100080, China

*Corresponding author. Fax: 86-10-62559373; tel: 86-10-62562821; e-mail: Hanbx@iccas.ac.cn.

Supporting Information

1. Experimental Section

Materials The surfactant cetyltrimethylammonium bromide (CTAB) and ethanol were provided by Beijing Chemical Reagent Company (A.R grade). n-Heptane supplied by Beijing Chemical Factory was A. R. grade. CO₂ (>99.99% purity) was provided by Beijing Analysis Instrument Factory. Tetraethyl orthosilicate (TEOS, A. R. grade) was supplied by Tianjin Yongda Chemical Reagent Center. Hydrogen tetrachloroaurate (HAuCl₄·3H₂O) was purchased from Shenyang Jinke Reagent Company. P-Nitrophenol was supplied by Science and Technology Development Company of Beijing Institute of Technology. Sodium borohydride (NaBH₄) (A. R grade) was produced by Beijing Chemical Reagent Company. Double-distilled water was used.

Effect of compressed CO₂ on the phase behavior of CTAB/n-heptane/water emulsions The apparatus for observing phase behavior of the emulsions was similar to that used previously.^[S1] The YKKY A2 digital temperature controller was used to control the temperature of the water bath. The accuracy of the temperature measurement was ±0.1 K. The pressure gauge used was composed of a pressure transducer (FOXBORO/ICT, Model 93) and an indicator, which was accurate to ±0.025 MPa in the pressure range of 0-20 MPa. In the experiment, a suitable amount of n-heptane, water and CTAB ([CTAB]=0.02 g/mL, water:oil (v/v)=1:1) were added into the viewing cell after the air in the cell was replaced by CO₂. The temperature of the system was controlled at 303.2 K. After the thermal equilibrium had been reached, CO₂ was charged into the autoclave under stirring until a suitable pressure was reached.

Synthesis of hollow silica nanospheres in water/n-heptane/CTAB emulsions The apparatus for synthesizing hollow silica nanospheres in the emulsions with compressed CO₂ was similar to that used for observing the phase behavior described above. It consisted mainly of a view cell with stirrer, a high-pressure pump, a constant temperature water bath, and a pressure gauge. In the experiment to prepare the hollow silica spheres, the desired amount of tetraethyl orthosilicate (TEOS) was charged into the high pressure view cell that contained n-heptane, water and CTAB ([CTAB] = 0.02 g/mL, V_{TEOS}:V_{heptane} = 1:4, 1:9, or 1:19, V_{oil}:V_{water} = 1:1) under stirring at 303.2 K. CO₂ was charged into the view cell to suitable pressure, and the mixture was stirred for 24 h. After depressurization, the suspension in the cell was centrifuged and washed with double-distilled water and alcohol for several times. The sample was dried under vacuum for 24 h at 60 °C. The dried powder was heated to 550 °C in air with a rate of 1°C/min and calcined at this temperature for 6 h to obtain the final silica products. To prepare the silica in the absence of CO₂, HCl was used to keep the pH of the emulsion at 3.0 or 4.0. Other experimental procedures were similar to above.

Synthesis of the Au/silica nanocomposites 1 mg of the hollow silica sphere powder with ordered mesoporous walls prepared at 3.91 MPa using the above method with TEOS to heptane volume ratio of 1:9 was dispersed in 1 mL water. After 5 min of sonication, the solution was mixed with 2 mL of 0.5 wt% HAuCl₄ solution. The mixture was stirred for 48 h, allowing the Au precursor entering into the pores of the silica spheres. Then 1 mL of 1M NaBH₄ solution was added to reduce the Au³⁺. The precipitate was washed with water until the solution became colorless. Then the Au/silica composites were dried at 60°C for 24 h under vacuum.

Reduction of p-nitrophenol catalyzed by the Au/silica nanocomposites 0.2 mg of the Au/silica nanocomposites prepared above was added into 2 mL of 1 M NaBH₄ aqueous solution, and the mixture was stirred for 30 min at room temperature. 2 mL of 3 × 10⁻³ M p-nitrophenol was added into the mixture that was stirred. The p-nitrophenol was reduced to p-aminophenol by NaBH₄ in the presence of the catalyst, and the deep yellow color of solution became light with the reaction going on, and became colorless after the reaction was completed. The progress of the reaction was monitored by determining the UV-vis spectra of the solution at different reaction times, and a TU-1901 Model spectrophotometer produced by Beijing Purkinje General Instrument Co. Ltd was used.

Characterizations The morphology of the particles obtained were characterized by SEM (TECNAI 20 PHILIPS electron microscope) equipped with EDAX. The structure of the products was studied by TEM (JeoL-1010) operated at 100 kV. The sample was dispersed in ethanol, and then deposited on the copper grid. Powder XRD analysis of the samples was performed on an X-ray diffractometer (Model X'Pert PRO) with Cu Ka radiation. Thermogravimetric analysis was carried out on a PerkinElmer TGA instrument. The temperature range was from 16 to 800 °C with a heating rate of 10 °C/min, and the experiments were carried out in nitrogen atmosphere. The porosity properties of the obtained silica were determined by nitrogen adsorption-desorption isotherm using a Micromeritics ASAP 2020M system. The pore size distribution was calculated from the adsorption isotherm curves using the Brunauer-Joyner-Halenda (BJH) method. The IR spectra of the sample were recorded on an TENSOR 27 IR spectrometer. The UV-Vis absorption study of the samples was performed on a TU-1901 Model spectrophotometer. The powders were first dispersed in ethanol and the spectrum was measured. ²⁹Si MAS NMR spectrum was recorded on a Bruker DMX-400 spectrometer. The samples were fitted in a 7 mm ZrO₂ rotor, spinning at 10 kHz.

2. Results and discussion

Effect of CO₂ pressure on the properties of CTAB/n-heptane/water emulsions Figure S1 shows the photographs of the CTAB/n-heptane/water emulsions at different CO₂ pressures under stirring. In the absence of CO₂, the emulsion was turbid because the droplet size was large. The emulsion was transparent at CO₂ pressure of 3.91 MPa, indicating the formation of nanoemulsion that has very small and uniform dispersed droplets.^[S1] At other pressures the emulsion was turbid because the droplet size was large. In our experiment conditions, the volume expansion of the system was about 15% after adding the CO₂.

SEM-EDAX SEM-EDAX shown in Figure S2 indicated clearly the presence of silica.

²⁹Si NMR The magic angle spinning ²⁹Si NMR spectrum of the calcined hollow silica nanospheres is shown in Figure S3. The main observed bands are centered at chemical shifts of δ = -92.7, -103.2, and -111.0 ppm. These components are assigned to silicon with different numbers of Si neighbors in the second coordination sphere, namely Q₂ [Si(OSi)₂(OH)₂], Q₃ [Si-(OSi)₃(OH)₁], and Q₄ [Si(OSi)₄], respectively. The ratio between the peak areas of Q₃ and Q₄ is a measure of the degree of cross-linking of the silica network. From the relative peak areas, the ratio of these species is Q₂:Q₃:Q₄ = 0.07 : 0.58 : 1, indicating the presence of terminal hydroxyl groups in the shells.

Thermogravimetric analysis Figure S5 shows thermogravimetric analysis (TGA) curves of the silica hollow spheres synthesized before and after calcination. The experiment was conducted under nitrogen atmosphere with a heating rate of 10°C/min. For the uncalcined sample, the weight loss at the beginning is likely due to the desorption of the adsorbed water. It eliminates about 5% of its weight in the temperature range of 25–100 °C. The loss of 25 % centred at 225 °C is attributed to removal of surfactant from the silica sphere shells. The loss of about 10% weight in the temperature range of 250–550 °C is related to removal of water from the condensation of terminal silanol groups. For the calcined sample, the weight lost is 7.6% below 100°C due to the adsorbed water, and no other weight loss in the curve.

FT-IR study The FT-IR spectra of samples obtained before and after calcination are shown in Figure S6. The peaks around 1700 and 3430 cm⁻¹ correspond to the carboxyl and hydroxyl groups, respectively. Carboxyl peak appeared from the atmospheric carbon dioxide. The bands at 1090 cm⁻¹, 960 cm⁻¹, 800 cm⁻¹, and 470 cm⁻¹ are attributed to the asymmetric stretching vibrational mode of Si-O-Si, stretching vibration of Si-OH, symmetric stretching of bulk Si-O-Si, and bending modes of bulk Si-O-Si, respectively.^[S2, S3] The weak peaks at 2855 and 2920 cm⁻¹ in the spectrum of the as-synthesized sample (before calcination) belong to the stretching vibrations of C-H bonds, which show that a few organic groups are adsorbed on the spheres. It indicates that surfactant CTAB exists in the as-synthesized sample. It is confirmed by the TGA analysis in Figure S5. The IR spectra of the silica spheres obtained at the other pressures are nearly the same with that shown in Figure S6.

BET measurement of the sample before calcination Figure S7 shows N₂ adsorption-desorption isotherms of the hollow silica spheres before calcination. The BET surface area, pore volume, average pore size were 339.8 m²·g⁻¹, 0.3728 cm³·g⁻¹, 2.8 nm, respectively.

The effect of the TEOS concentrations At other TEOS/heptane ratios, monodisperse and uniform hollow silica spheres with ordered mesoporous shells were also obtained at 3.91 MPa. The TEM images of typical particles obtained at TEOS/heptane ratios of 1:4 and 1:19 are given in Figure S8. It is clearly seen that the shell thickness of the silica spheres increased with increasing the amount of the Si precursor in the dispersed nonpolar droplets. The shell thicknesses of the hollow silica spheres obtained at TEOS/heptane ratios of 1:4 (Figure S8a), 1:9 (Figure 1c) and 1:19 (Figure S8b) are about 30 ± 3 nm, 20 ± 3 nm, and 10 ± 2 nm, respectively, indicating that the thickness of the mesoporous shells of the monodisperse uniform spheres can be controlled by the concentration of the Si precursor in the oil droplets.

The silica particles obtained without CO₂ In the CO₂ pressure range, the pH value of aqueous phase is in the range of 3.1-3.9 because ionization of CO₂ in water.^[S4] We also prepared the silica using the same method without using CO₂. In the experiments, the pH of the emulsion was controlled at 3.0 or 4.0 by adding HCl. The hollow silica spheres were not obtained in the absence of CO₂, but the particles with the ordered pore channels could be formed. Figure S9 shows the TEM image of the sample prepared at pH=3.0, and that fabricated at pH=4.0 was similar.

Small angle X-ray diffraction study Figure S10a shows the small angle X-ray diffraction patterns of the calcined hollow microspheres obtained at different CO₂ pressures. The three Bragg diffraction peaks can be assigned to the (100),

(110) and (200) reflections of a hexagonal symmetry structure (P6mm). For the spheres prepared at 2.50 MP, 3.91 MPa, and 5.01 MPa, the $d(100)$ spacing calculated from the XRD data is 3.6 nm, 4.3 nm and 4.8 nm, respectively. Figure S10b indicates the $d(100)$ spacing increased nearly linearly with CO₂ pressure.

Characterization of Au/silica nanocomposites and catalytic reaction Figure S11 shows the XRD pattern of the Au/silica composite. The four diffraction peaks correspond to the 111, 200, 220, 311 planes, corresponding to a typical pattern of standard face-centered-cubic Au. The broadened diffraction patterns indicate that the small size of Au nanocrystals are obtained. As shown in Figure S12a and S12b, the Au/silica nanocomposites kept the structure of hollow silica spheres. The Au nanoparticles existed in the pore channels (red signs) and outside the channels. The electron-diffraction pattern (Figure S12c) showed characteristic rings of polycrystalline Au and corresponded to standard face-centered-cubic Au, which was consistent with the XRD results (Figure S11). The UV-vis spectrum of Au/silica nanocomposites, as shown in Figure S13, showed a quite broad absorption peak with a λ_{\max} at 550 nm. This is attributed to the plasmon band of Au(0).

p-Aminophenol is an important chemical and can be produced by reduction of p-nitrophenol by NaBH₄ using gold particles as the catalysts.^[S5, S6] The Au/silica nanocomposites prepared were employed as the catalyst for this reaction. The reactant p-nitrophenol and product p-aminophenol have absorption at 400 nm and 300 nm, respectively, and UV-vis spectrum determination is a commonly used method to monitor the reaction. Figure S14a shows typical UV-vis spectra of the reaction mixture. The reaction did not occur in the absence of the catalyst. In the presence of the composites, the absorption at 400 nm decreased and that at 300 nm increased with reaction time, and the UV-vis absorption at 400 nm disappeared within 0.5 h, indicating that the catalyst was very effective. Figure S14b shows that $\ln(C_t/C_0)$ changed linearly with reaction time (C_t and C_0 are p-nitrophenol concentrations at time t and $t=0$, respectively), which was obtained from the absorbance of p-nitrophenol.

The reusability of the Au/silica nanocomposite catalyst was tested. After reaction, the used catalyst was separated by centrifugation, washed, dried, and then reused in the next run. Table 1 gives the time for complete reaction of the p-nitrophenol in each run. The catalyst remained high activity after reused for five times. The morphology of the Au/SiO₂ nanocomposites after 5 recycling was similar to that the composites before reused, indicating that the catalyst was not only very active, but also very stable.

References

- [S1] J. L. Zhang, B. X. Han, C. X. Zhang, W. Li, X. Y. Feng, *Angew. Chem. Int. Ed.* 2008, **47**, 3012.
- [S2] M. M. Mohamed, T. M. Salama, T. Yamaguchi, *Colloid Surf. A* 2002, **207**, 25.
- [S3] P. Cheng, M. P. Zheng, Y. P. Jin, *Mater. Lett.* 2003, **57**, 2989.
- [S4] D. X. Liu, J. L. Zhang, B. X. Han, J. F. Fan, T. C. Mu, Z. M. Liu, W. Z. Wu and J. Chen, *J. Chem. Phys.*, 2003, **119**, 4873.
- [S5] G. Y. Liu, H. F. Ji, X. L. Yang, Y. M. Wang, *Langmuir* 2008, **24**, 1019.
- [S6] J. Lee, J. C. Park, H. Song, *Adv. Mater.* 2008, **20**, 1523.

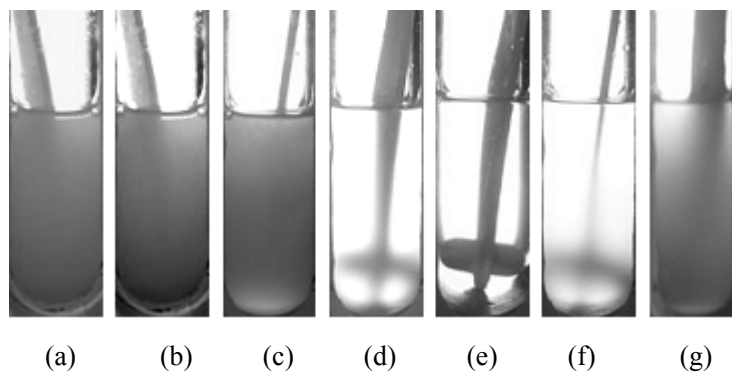


Figure S1. Photographs of H₂O/CTAB/n-heptane system ([CTAB] = 0.02 g/mL, water:oil (v/v) = 1:1) at 303.2 K and CO₂ pressures of 0 MPa (a), 1.26 MPa (b), 2.50 MPa (c), 3.70 MPa (d), 3.91 MPa (e), 4.11 MPa (f), 5.01 MPa (g) under stirring.

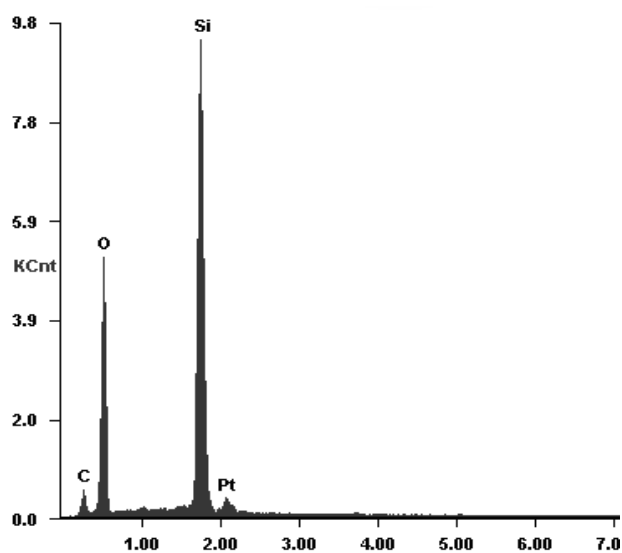


Figure S2. SEM-EDAX of calcined silica obtained in the CTAB/n-heptane/water nanoemulsions induced by CO₂ ([CTAB] = 0.02 g/mL, V_{TEOS}:V_{heptane} = 1:9, V_{oil}:V_{water} = 1:1, P = 3.91 MPa, 24 h, 303.2 K).

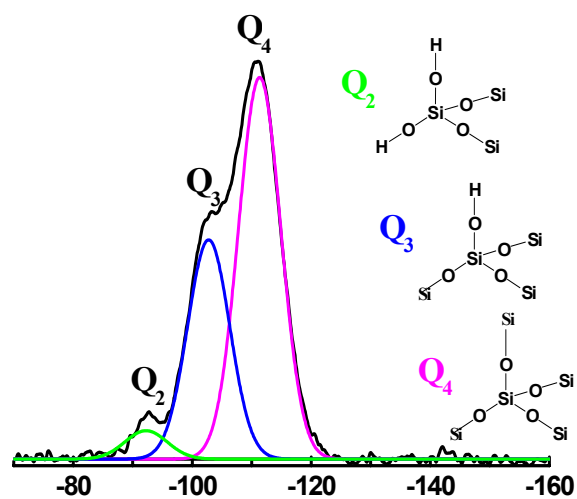


Figure S3. ^{29}Si MAS NMR spectrum of the calcined silica nanospheres. The experimental conditions was the same as that in Figure S2.

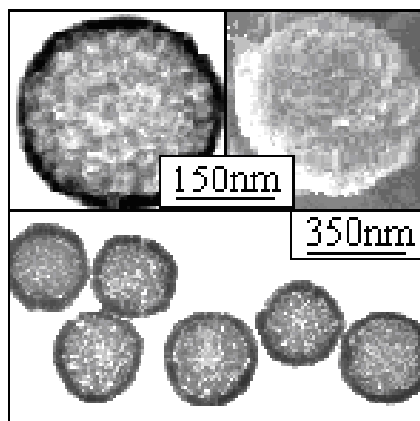


Figure S4. The TEM image of the hollow spheres obtained before the calcination, and the insets are the TEM (right) and SEM (left) images of a typical sphere.

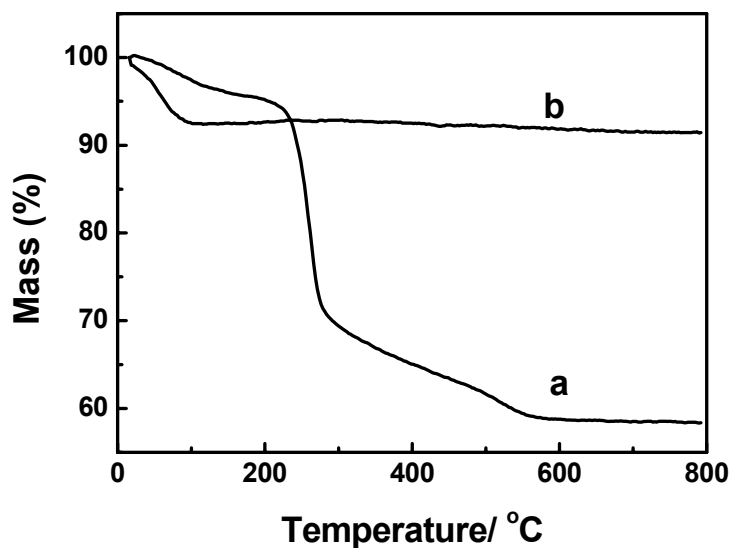


Figure S5. The thermogravimetric analysis (TGA) plots of the silica spheres obtained before (a) and after (b) calcination. Experimental condition was the same as that in Figure S2.

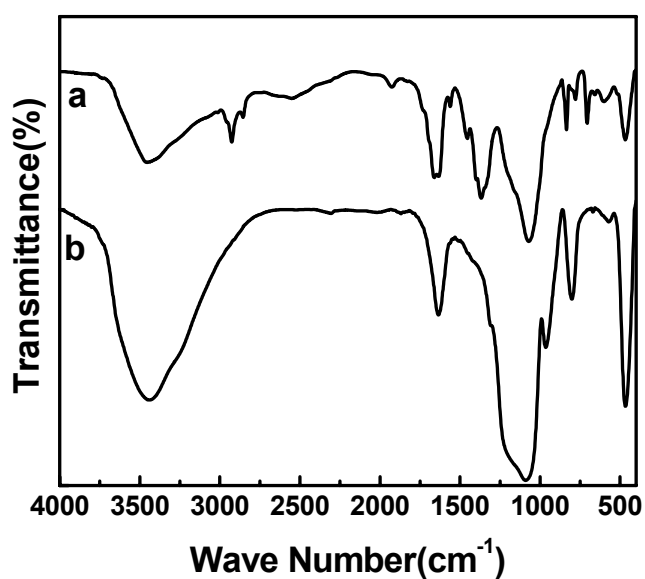
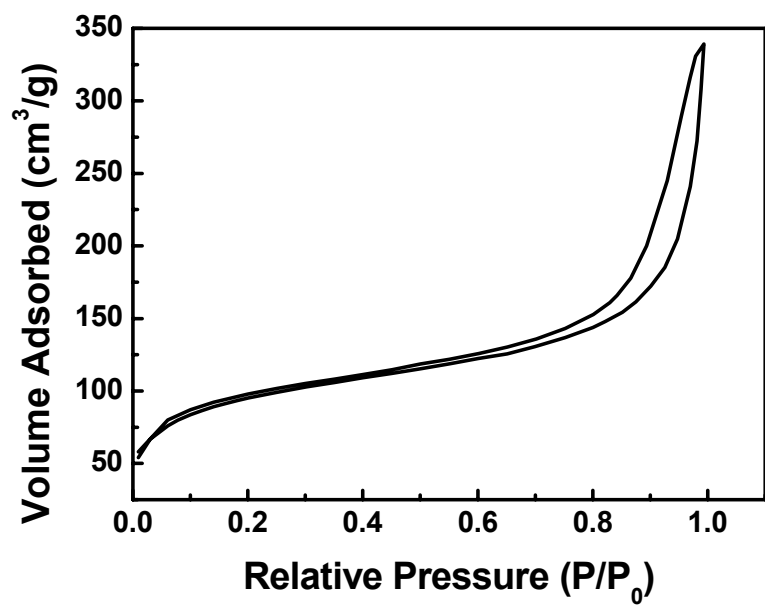
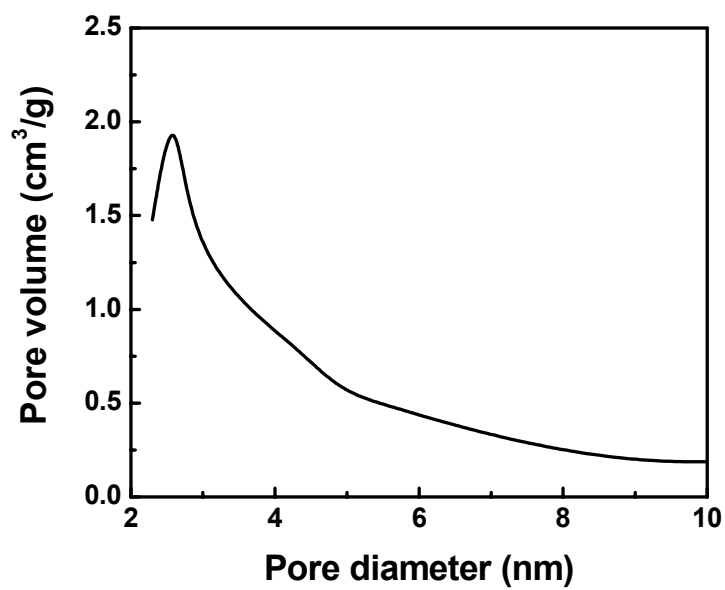


Figure S6. FT-IR spectra of the samples obtained before (a) and after (b) calcination. Experimental condition was the same as that in Figure S2.



(a)



(b)

Figure S7. N₂ adsorption–desorption isotherm (a) and pore-size distribution curve (b) of the hollow silica spheres before calcination. Experimental condition was the same as that in Figure S2.

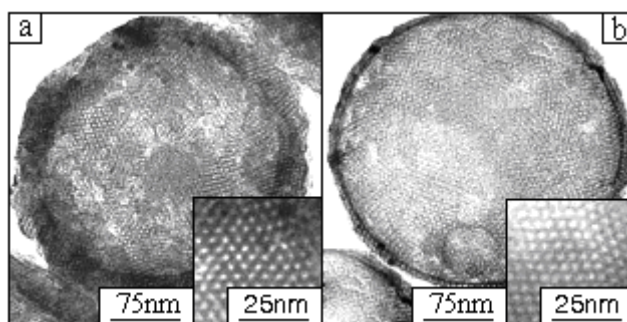


Figure S8. The TEM images of the calcined hollow silica spheres obtained at $V_{\text{TEOS}}:V_{\text{heptane}} = 1:4$ (a) and $V_{\text{TEOS}}:V_{\text{heptane}} = 1:19$ (b), respectively, and other experiment conditions were the same as that in Figure S2.

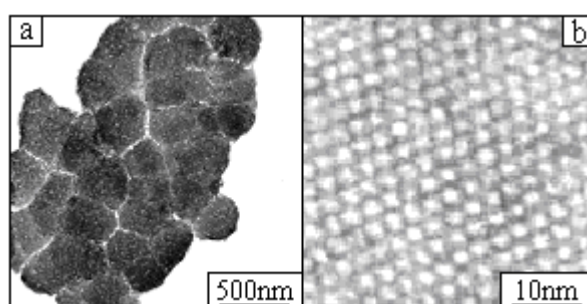
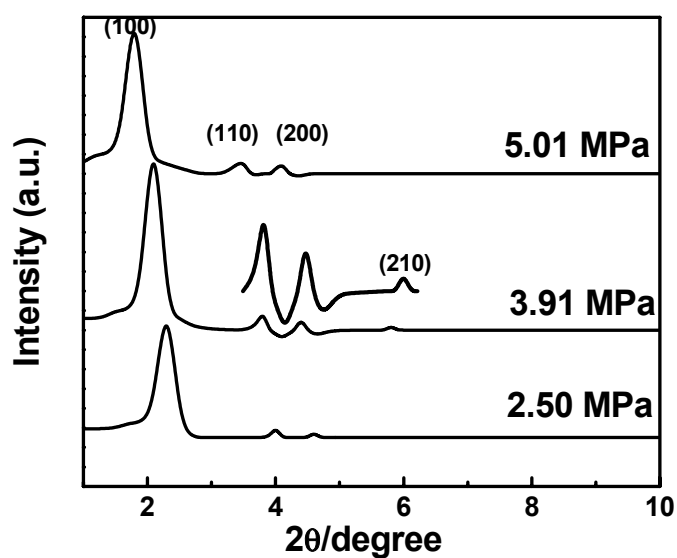
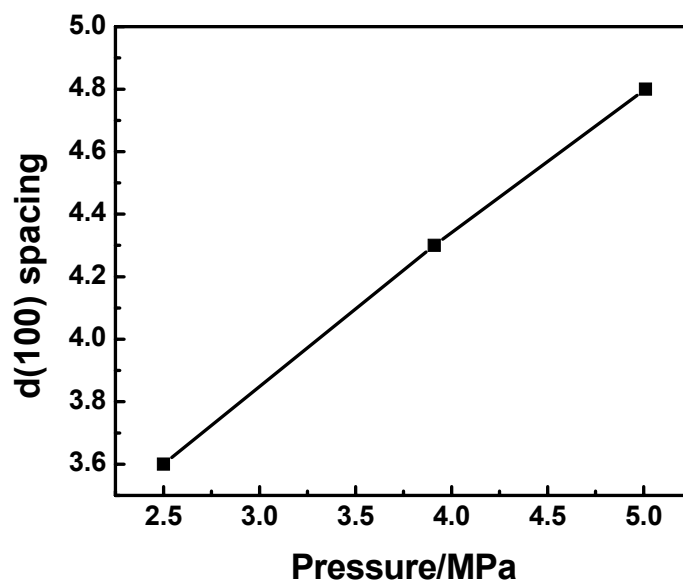


Figure S9. The TEM images of the silica particles obtained at pH=3.0 by adding HCl without CO₂. ([CTAB] = 0.02 g/mL, $V_{\text{TEOS}}:V_{\text{heptane}} = 1:9$, $V_{\text{oil}}:V_{\text{water}} = 1:1$, 24 h, 303.2 K).



(a)



(b)

Figure S10. (a) Small angle X-ray diffraction patterns of the hollow spheres obtained at different pressures; (b) the d(100) spacing of the hexagonal arrays at different pressures. Experimental condition was the same as that in Figure S2.

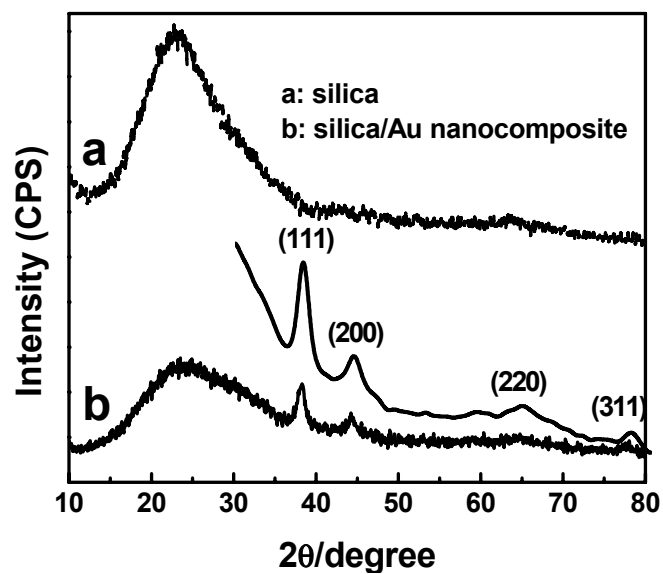


Figure S11. Powder X-ray diffraction patterns of silica hollow spheres (a) and Au/silica nanocomposites (b) in the wide-angle region. Experimental condition was the same as that in Figure S2.

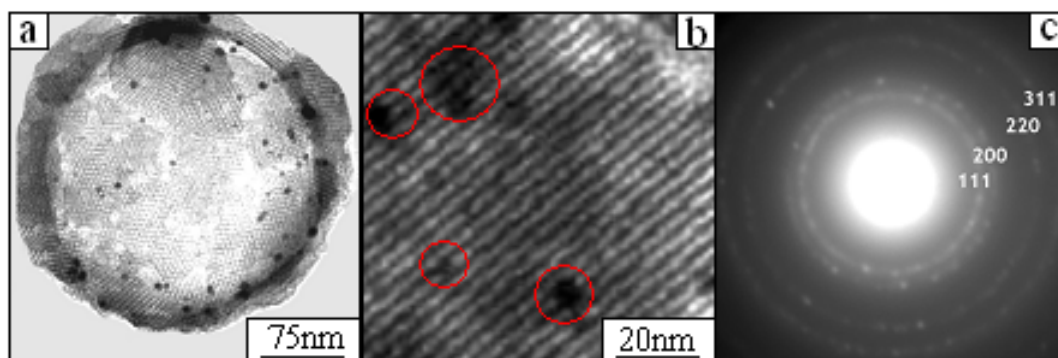


Figure S12. TEM image (a), high-magnification TEM image (b) and the electron-diffraction pattern (c) of Au/silica nanocomposites. Experimental condition to prepare the hollow silica spheres was the same as that in Figure S2.

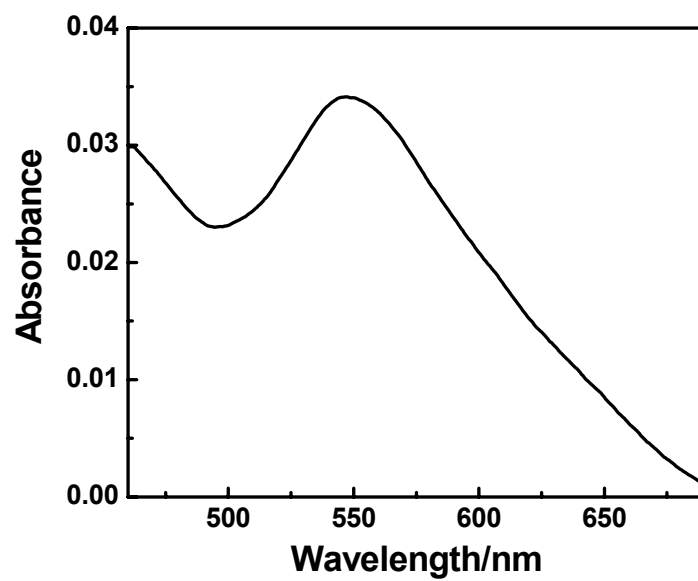
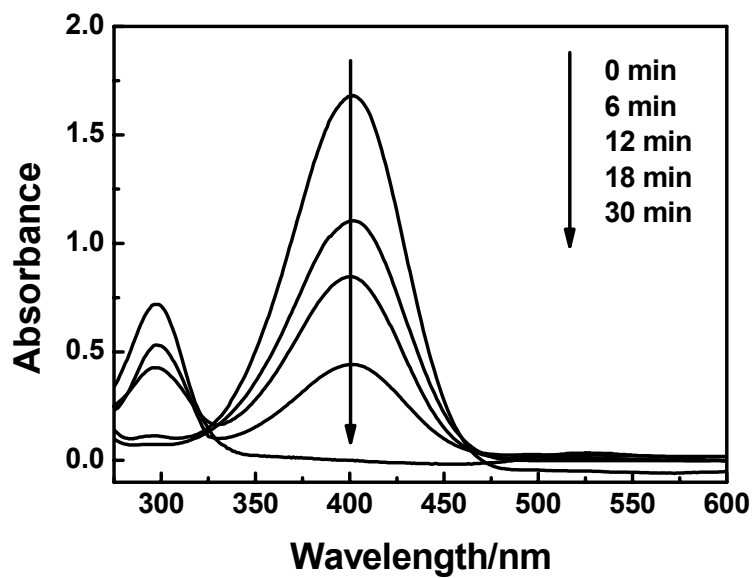
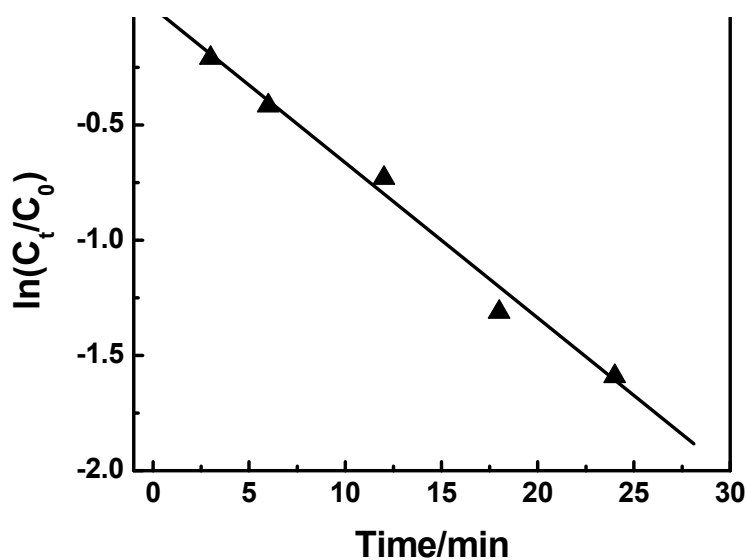


Figure S13. UV-vis spectrum of the Au/silica nanocomposites alcohol solution. Experimental condition to prepare the hollow silica spheres was the same as that in Figure S2.



(a)



(b)

Figure S14. (a) Time-dependent UV-vis spectra changes of the reaction mixture catalyzed by Au/silica nanocomposites; (b) Plot of $\ln(C_t/C_0)$ versus time. Experimental condition to prepare the hollow silica spheres was the same as that in Figure S2.

Table 1. Time required for complete reaction of p-nitrophenol in each run of reusing the catalyst.

Run No.	1	2	3	4	5
Reaction time (min)	30	30	30	33	33